DEVELOPMENT OF THE NEW ELF/VLF RECEIVER FOR DETECTING THE SUDDEN IONOSPHERIC DISTURBANCES

Le MINH TAN[1] , Keyvan GHANBARI[2]
[1]*Department of Physics, Faculty of Natural Science and Technology, Tay Nguyen University*
567 Le Duan Street, Buon Ma Thuot City, DakLak Province, 630000, Vietnam, +84935318151, Email: lmtan@ttn.edu.vn
[2]*Energy Engineering and Physics Department, Amirkabir university of technology, 15875-4413, Tehran, Iran*

Abstract: The Extremely Low Frequency (ELF; 3 – 3000 Hz) and Very Low frequency (VLF; 3 – 30 kHz) technique is useful for studying the D-region ionosphere of the Earth. Based on our previous receiver, we developed a new ELF/VLF receiver with three main parts: loop antennas, amplifier and data logger. The antenna includes two loops which are right isosceles triangles with the base of 2.6 m. Each loop consists of 8 turns of 18 AWG copper wire. A surface of one loop orients the direction of North - South, the surface of other loop orients the direction of East - West. The developed amplifier with two channels has the flat frequency response in the frequency range of 1 – 20 kHz. The amplified signals are digitized by a standard sound card with the sampling rate of 96 kHz and calibrated by 1 PPS of the GPS receiver. UltraMSK software has been used to detect the Sudden Ionospheric Disturbances (SIDs). To demonstrate the ability of instrument, we recorded and analyzed the SID events during 2013 - 2014 at a low-latitude station, Tay Nguyen university (TNU), Vietnam (Geog. 12.65^o N, 108.02^o E). The results in the daytime Wait's parameters are in accordance with the other authors' results.

Keywords: *ELF/VLF receiver, frequency response, EIWG, tweek atmospherics, solar flares, SIDs, Wait's parameters.*

I. INTRODUCTION

The D region is the lower ionosphere which is below about 95 km. This region has the high pressure, which is important for the photochemical reactions. It also has many ionization sources which contribute to the ion productions [1]. The conductivity of the D-region ionosphere increases exponentially with the height. The electron density (N_e) as a function of altitude (h) is determined from the Wait's parameters, the reference height h' (in km), and the exponential sharpness factor β (in km^{-1}) [2]:

$$N_e(h) = 1.43\times10^{13}\exp(-0.15h')\exp[(\beta-0.15)(h-h')] \qquad (1)$$

The Extremely Low Frequency (ELF, 3 – 3000 Hz) and Very Low Frequency (VLF, 3 – 30 kHz) waves are generated from the transmitters installed by man or from natural resources such as lightning, earthquakes, volcanic eruptions, etc. There are many VLF transmitters in the world which serve the navigation, positioning and research. If the disturbances of these signals are detected by the receivers, we can investigate the characteristics of the ionosphere [3]. Many VLF signals of the transmitters are modulated by MSK (Minimum Shift Keying). The VLF signals can propagate in the environment between the D region and the ground called the Earth-Ionosphere waveguide (EIWG) with the low attenuation in the range of 0.5 - 2 dB/Mm [4].

Recently, some narrowband receivers with low price are developed, but their software only record the intensity of signals and do not record the phase of the signals. Moreover, the signal strength is obtained in the form of the relative ratio between the signal and the background noise, which is not suitable for data input of the Long Wave Propagation Capability (LWPC) program to calculate the ionosphere's parameters. There are some receivers which are used for research. However, they have a relatively high cost and need to be installed at the really quiet places.

In the previous works, we designed a broadband ELF/VLF receiver with one channel to record the electromagnetic pulses radiated from lightning discharges. It was installed at Tay Nguyen University (TNU), Vietnam to investigate the nighttime D-region ionosphere [5, 6]. In present work, this receiver has been developed with two channels to record the narrowband signals for studying the effects of solar flares on the D-region ionosphere. Recording the perturbations of both amplitude and phase of VLF waves, the D region's characteristics and its parameter changes will be determined, which serves the forecasting and modeling activities.

The development of receiver meets the criteria of a good ability for removing the interferences, a low cost and the advantages for observing the D-region ionosphere. In this paper, we discuss some experimental results to demonstrate the ability of the receiver in the study of the ionosphere.

Manuscript received October 3, 2015; revised February 15, 2016

II. DEVELOPMENT OF ELF/VLF RECEIVER

Figure 1 shows the diagram of the developed ELF/VLF receiver. It consists of a magnetic antenna, a pre-amplifier, a service unit (SU), a GPS receiver and Data acquisition.

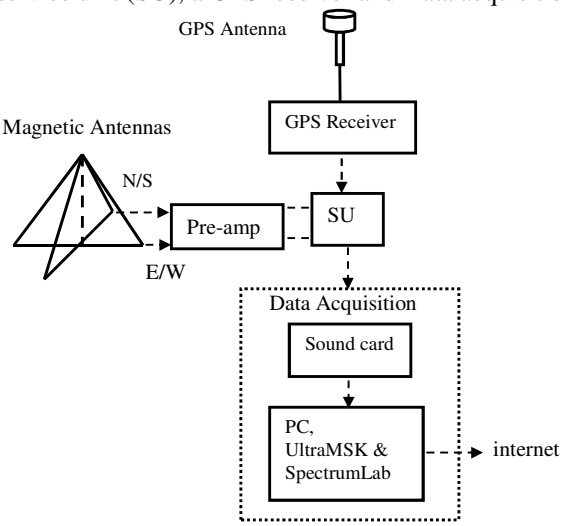

Figure 1. The diagram of the new ELF/VLF receiver.

2.1. Development of orthogonal loop antenna

We designed the magnetic antenna including the orthogonal loops. Its shape is a right isosceles triangle with the base of 2.6 m (Figure 2). Each loop has 8 turns of 18 AWG copper wire. These loops are installed with the North-South (N/S) and East-West (E/W) directions. The measured resistance of one loop is about 1.2 Ω and its inductance is about 0.57 mH. The voltage will be induced in the loop if the magnetic field of the electromagnetic wave changes and passes to the antenna [7]. The output voltage is given by Faraday' law [8]:

$$V = j2\pi fNAB\cos\theta \qquad (2)$$

Where, V is the output voltage, N is the number of turns in the antenna, A is area of the antenna (in m^2), B is the magnetic flux density (in T), and θ is the angle of the magnetic field from the axis of the loop. The response pattern of the antenna is a dipole in azimuth because the axis of the loop is horizontal.

The normalized antenna sensitivity (S_o) is calculated by following equations [8],

$$S_o = \frac{c(4kTR_a)^{1/2}}{2\pi NA} \qquad (3)$$

Where, $A = 1.69$ m^2 is an area of the loop, R_a is the loop dc resistance, $N = 8$ is the number of turns, $c = 2.998$ x10^8 ms^{-1} is the speed of light, $k = 1.38$ x10^{-23} JK^{-1} is Boltzmann's constant, T is the temperature in Kelvins. At room temperature, we have $4kT = 1.61$ x10^{-20} J. Therefore, the normalized sensitivity of this antenna is 4.91 x10^{-4} $V/Hz^{-1/2}$ m^{-1}. This value is smaller than that of square antenna with the base of 56.7 cm and 21 turns of 18 AWG wire ($S_o = 8.96$ x10^{-4} $V/Hz^{-1/2}m^{-1}$) [8]. It means that our loop is more sensitive than that of this antenna.The bigger antenna has the higher sensitivity. It means that it is sensitive to the noise sources. The selected antennas are small in size for the limiting of the high noise of the city. In order to prevent the interferences due to the high frequency waves, the loops are covered with silver shields. The loop antenna has been chosen because it can be easily designed with two directions. The loop facing the North-South is better for VLF signals from transmitters, whereas the loop facing the East-West is more sensitive to sferics [8, 9].

Figure 2. Right isosceles triangle antennas with N/S and E/W directions.

2.2. Development of the pre-amplifier

Figure 3a shows the one-channel circuit diagram of pre-amplifier which has two stages. The first stage is a low pass filter which contains an RC cell (R3 and C3). The second stage has a low-pass filter which contains an RC cell (VR and C6) and a high-pass filter with C4 and R4. The details of this circuit were described in the previous work [6]. In this work, the pre-amplifier has been added another channel.

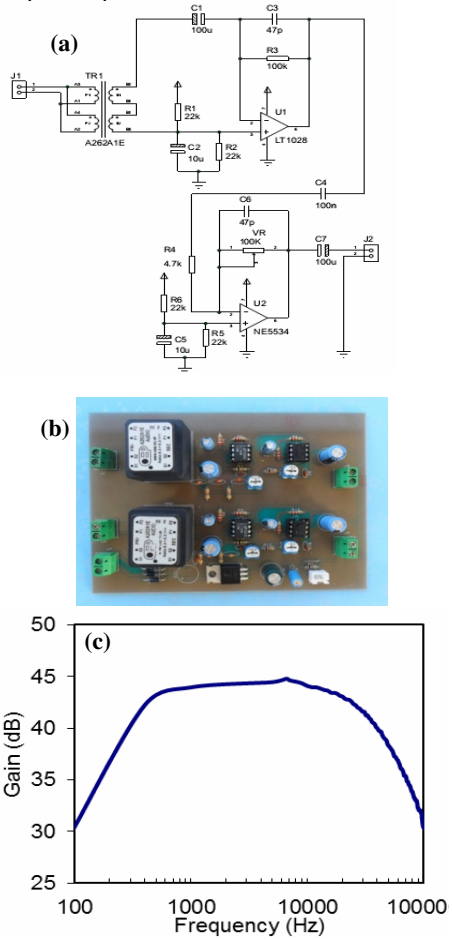

Figure.3. The circuit diagram of one-channel pre-amplifier (a), PCB after being assembled with the electronic components (b) and frequency response (c).

The developed circuit layout is designed by using Protues V7.10 software, and then the printed circuit board (PCB) is also made. Figure 3b shows the PCB after being assembled with the electronic components. The calibration for the pre-amplifier was presented in our previous work [6]. Figure 3c shows the frequency response of the pre-amplifier. The 3 dB points appear at ~ 400 Hz on the low side and at ~ 40 kHz on the high side. The flat frequency response is in the frequency range of 1 kHz to 20 kHz.

2.3. Installation of the ADC and software

The analog signal from amplifier is digitized by an ADC. The sound card, M–audio delta 44, is used as an ADC. This sound card has a 4-input, 4-output digital recording interface. It provides the highest quality digital audio available - all up to 24-bit data width and any sampling rate from 8 kHz to 96 kHz. It also has a wide dynamic range of 103 dB. The gain of the pre-amplifier is adjusted such that the output voltage falls between ± 5 volts to prevent clipping at the ADC. The amplified VLF signals from the pre-amplifier go into the first input of the sound card. The second input of sound card is provided 1 PPS (pulse per second) of the GPS with the accuracy from 100 – 1000 ns.

The precise sampling frequency of the sound card is calibrated using 1 PPS to obtain a reliable center frequency for the quadrature-phase mixer [3]. The HP Z3816A GPS receiver is used to provide 1PPS with the width of pulses of 20 microseconds. These pulses are converted by an integrated circuit (Figure 4a) in SU to the pulses with the width of 10 microseconds. The screens of the oscilloscope show the 1 PPS before being integrated and a zoomed pulse after being integrated (Figure 4b, c).

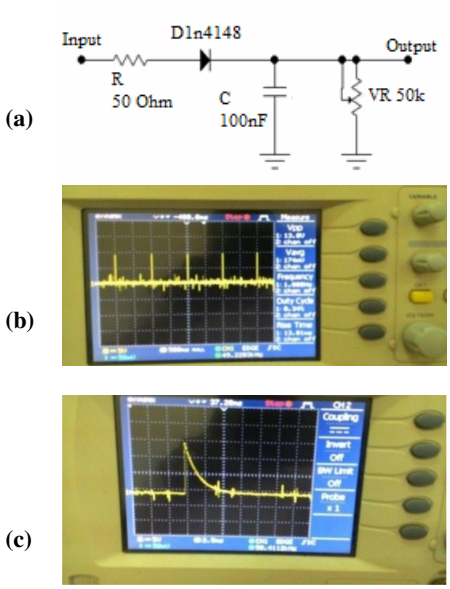

Figure 4. The diagram of the integrated circuits (a), the showing of the oscilloscope's screen of 1 PPS before being integrated and a zoomed pulse after being integrated (c).

UltraMSK software developed by James Brundell is used to record the VLF signals from the transmitters. The PC runs under the Linux operating system. The PC is connected to internet and its clock is set to within +/- 500 milliseconds of UTC by using the Network Time Protocol. The VLF signals are detected by a quadrature-phase mixer which splits and mixes the received signal with an in-phase component on one hand and a quadrature-phase component on the other. After demodulating signal, the two components are compared and information relating the phase and amplitude of the VLF signal is extracted [3].

III. SOME EXPERIMENT RESULTS

Figure 5 shows a spectrum for the N/S channel at 8:14 UT on 26 April, 2014. The VLF signals are marked by arrows. The NWC/19.8 kHz and NAA/24.0 kHz signals are modulated with MSK (minimum shift keying) and JJI/22.2 kHz signal is modulated with FSK. On this spectrum, there is a broader hump visible in the 1.4 kHz – 27 kHz range as a result of the radiation from lightning discharges. We chose the stable NWC signal to detect the SID events.

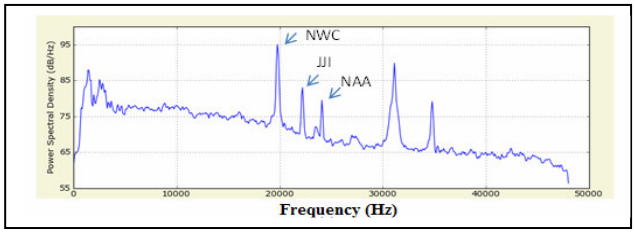

Figure 5. Spectrum for N/S channel on 26 April, 2014 at 8:14 UT.

Figure 6 shows the diurnal variations of the VLF signals which propagate to TNU, Vietnam and DAISY (1.37° N, 103.8° E), Singapore on 13 February, 2014. The perturbation events of the VLF signals are compared with the intensity of X-ray flux recorded by the Geostationary Operational Environmental Satellite (GOES). The VLF signal of the NWC-TNU path significantly responds to solar flares with classes of C3.6, C8.4, M1.0 and M1.7. Solar flares on 13 February cause the strength and phase of the NWC signal to increase suddenly. The dips labeled as SS and SR occur on the signals during the sunset and sunrise transitions.

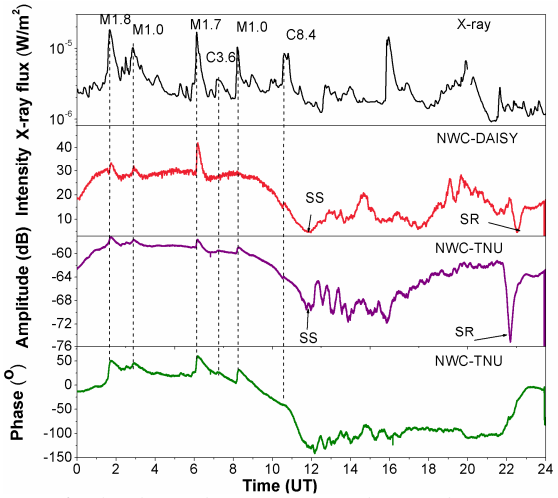

Figure 6. The diurnal variations and perturbations of the NWC recorded at TNU and DAISY on 13 February 2014.

During 2013-2014, there are 6 solar flare events which the signal amplitudes drop after the peaks to be below the

initial values. The signals then slowly recover with a long period of time. The flares with classes of M2.9, M5.0 and X1.1 which the peaks of X-ray flux occur at 3:02 UT on 25 October, 5:23 UT on 3 November and 4:26 UT on 8 November, 2013. The M2.9, M5.0 and X1.1 flares are presented in Figure 7 a, b, c, respectively. After the maximum perturbations, the VLF amplitudes reduce to be lower by 1 – 2 dB as compared to the normal values. Figure 7 d, e, f present the enhancements of the VLF signals due to flare classes of M1.5, M2.3 and M2.2 which the peaks of X-ray flux occur at 4:09 UT on 28 January, 2:57 UT on 14 February, and 2:16 UT on 27 December 2014, respectively. After the peaks of the signals, the amplitudes reduce about 0.5 dB. The responses of the NWC signal recorded at TNU are compared with those recorded by SID monitor at DAISY. The effects of solar flares on the NWC-DAISY path are nearly similar to those on the NWC-TNU path.

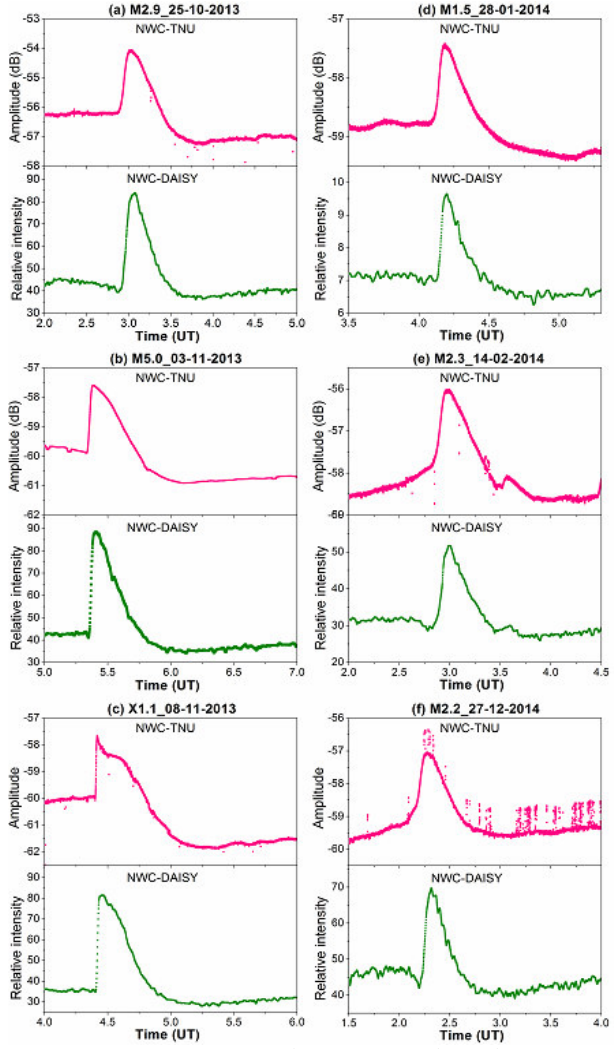

Figure 7. Responses of the VLF signals to the intense solar flares during 2013 - 2014.

The formation of the drops after the maximum disturbances in the NWC amplitude is explained by the modal interference pattern. The distance between the transmitter and receiver, as well as the temporal changes of the ionospheric parameters, affects on the shape of the VLF signals as a result of the shifts in the modal interference pattern. These shifts cause the amplitudes of the signals to drop below the unperturbed levels [3].

During 2014, we recorded 90 solar flare events and used the LWPC program to estimate the h' and β. The changes of them with the peaks of X-ray intensity are shown by Figure 8. When the X-ray intensity increases, the h' decreases from 72.83 to 60.88 km and the β increases from 0.31 to 0.53 km^{-1}.

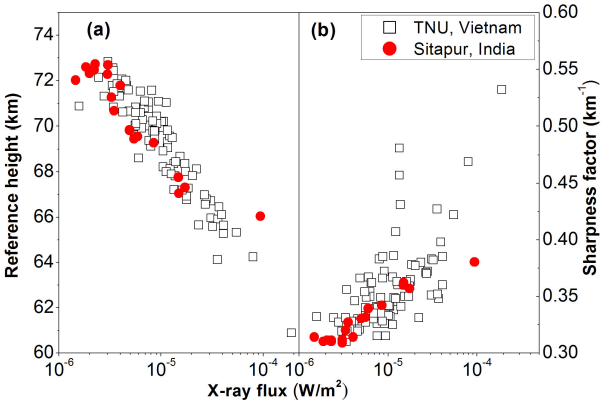

Figure 8. The variations of the Wait's parameters as a function of the peaks of X-ray intensity.

Our results in h' and β are compared with those reported by Basak & Chakrabarti [10]. These authors recorded 22 solar flare events with the zenith angle of 14° – 33° at Sitapur (22.45° N, 87.75° E), India. Considering the same series of solar flares, the changes of Wait's parameters in our work are in accordance with the findings reported by these authors [10]. The values of β in our work strongly scatter due to seasonal factors and large changes of the zenith angle (Figure 8b). The sunset and sunrise transitions also affect significantly on the changes of β.

IV. CONCLUSIONS

Based on the UltraMSK system and the previous ELF/VLF receiver with one channel, we developed the new receiver with two channels. The square antenna of the previous receiver is replaced by the right isosceles triangle antennas with N/S and E/W directions. We also added the second channel for the pre-amplifier and used 1PPS from the GPS to calibrate the ADC of the sound card, M-audio Delta 44. The improvement is useful to record the narrowband VLF signals. Our receiver can detect the amplitude and phase of the VLF signals. In addition, it has a low cost and can be easily installed.

We recorded the SID events during 2013 – 2014 and found that when intense solar flares occurred, our receiver clearly recognized the drops in the VLF intensity after the maximum disturbances on the NWC-TNU path. These phenomena are explained by the modal interference pattern. The increase of X-ray intensity causes the decrease of h' in the range of 72.83 – 60.88 km and the increase of β in the range of 0.31 – 0.53 km^{-1}. The results in the daytime Wait's parameters are in accordance with the findings of other authors.

Therefore, this developed receiver has enough quality to investigate the daytime D-region ionosphere. The new receiver can also be used to educate the students who are studying Space Science at TNU, Vietnam.

ACKNOWLEDGEMENT

We would like to thank John MacConnell for help on the installation of the GPS receiver. Special thanks the developer of UltraMSK, James Brundell for guiding the using of UltraMSK software. The authors acknowledge the X-ray data provided by the US National Geophysical Data Center. The authors also thank Stanford Solar Center for providing the VLF data.

REFERENCES

[1] R. D. Hunsucker, and J. K. Hargreaves, *The high-latitude ionosphere and its effects on radio propagation*, 1st ed., Cambridge University Press, New York, 2003.
[2] J. R. Wait, and K. P. Spies, *Characteristics of the Earth-ionosphere waveguide for VLF radio waves*, NBS Tech. Not, 1964.
[3] H. Dahlgren, T. Sundberg, B. C. Andrew, E. Koen, and S. Meyer, "Solar flares detected by the narrowband VLF receiver at SANAE IV", *S Afr J Sci*, vol. 107 (9/10), pp. 1- 8, 2011.
[4] J. A. Ferguson, and F. P. Snyder, *Approximate VLF/LF Waveguide Mode Conversion Model*, Technical Document 400, Naval Oceans Systems Center, San Diego, California, 1980.
[5] L. M. Tan, Observation of tweek atmospherics in Vietnamese low latitude region using a simple VLF receiver*, Procceedings of IEEE International Conference on Space Science and Communication*, Malaysia, pp. 219 – 223, 1-3 July 2013.
[6] L. M. Tan, M. Marbouti, K. Ghanbari, "Constructing A Low-Cost ELF/VLF Remote Sensing To Observe Tweek Sferics Generated By Lightning Discharge," *ACTA Technica Napocensis Electronica-Telecomunicatii*, vol. 56(2), pp. 1-5, 2015.
[7] S. Ramo, J. R. Whinnery and T. Van Duzer, *Fields and Waves in Communications Electronics*, John Wiley and Sons, New York, 1994.
[8] E. W. Paschal, *The design of broad-band VLF receivers with air-core loop antenna*, Stanford University, 1988. [Online]. Available: http://traktoria.org/files/radio/antenna/VLF/.
[9] G. T. Wood, *Geo-location of individual lightning discharges using impulsive VLF electromagnetic waveforms*, Ph.D. Thesis, Stanford University, Department of Electrical Engineering, 2004.
[10] T. Basak & S. K. Chakrabarti, "Effective recombination coefficient and solar zenith angle effects on low-latitude D-region ionosphere evaluated from VLF signal amplitude and its time delay during X-ray solar flares", *Astrophys. Space Sci.*, vol. 348(2), pp. 315-326, 2013.